scientific data

OPEN

DATA DESCRIPTOR

SpiDa-MRI: behavioral and (f)MRI data of adults with fear of spiders

Mengfan Zhang[1,2] ✉, Alexander Karner[1,2], Kathrin Kostorz[1], Sophia Shea[1], David Steyrl[1], Filip Melinscak[1], Ronald Sladky[1], Cindy Sumaly Lor[1,3] & Frank Scharnowski[1,3]

Neuroimaging has greatly improved our understanding of phobic mechanisms. To expand on these advancements, we present data on the heterogeneity of neural patterns in spider phobia combined with various psychological dimensions of spider phobia, using spider-relevant stimuli of various intensities. Specifically, we have created a database in which 49 spider-fearful individuals viewed 225 spider-relevant images in the fMRI scanner and performed behavioral avoidance tasks before and after the fMRI scan. For each participant, the database consists of the neuroimaging part, which includes an anatomical scan, five passive-viewing, and two resting-state functional runs in both raw and pre-processed form along with associated quality control reports. Additionally, the behavioral section includes self-report questionnaires and avoidance tasks collected in pre- and post-sessions. The dataset is well suited for investigating neural mechanisms of phobias, brain-behavior correlations, and also contributes to the existing phobic neuroimaging datasets with spider-fearful samples.

Background & Summary

Specific phobias are the most common anxiety disorders and can cause high levels of distress in affected individuals[1,2]. Spider phobia, defined as intense and exaggerated fear of spiders[3], is observed in a particularly large proportion of the population, with prevalence estimates ranging from 2.7% up to 9.5%[4–6]. With the help of neuroimaging, researchers can gain insights into the neural underpinnings of such specific phobias. Particularly functional magnetic resonance imaging (fMRI) has revealed brain correlates of emotions and psychological dimensions relevant to spider phobia (for a review see Hinze *et al.*[7]). Neuroimaging studies have identified a so-called "fear network" in the processing of spider-related stimuli, which consists of the amygdala, the insula, and the anterior cingulate cortex[7,8]. Other studies have suggested that disgust, which has been linked to the prevention of contamination[9–11], is associated with overlapping but distinct neural activation compared to fear[12]. As negative emotions, both fear and disgust are linked to avoidance behavior[13], which is a key symptom of anxiety disorders[3]. While phobic individuals tend to avoid the respective aversive stimulus, those who want to overcome their aversion may choose to approach the stimulus to expose themselves, resulting in an approach-avoidance conflict[14]. A variety of brain correlates of the approach-avoidance conflict have been proposed and include the inferior frontal gyrus, as well as the right dorsolateral prefrontal cortex (for details see Zorowitz *et al.*[15]). These findings can serve as a basis for further investigation of the specific underlying neural patterns in spider-phobic individuals[16]. Importantly, spider phobia is not a uniform condition[17]. Individuals with spider phobia may have different levels of fear, disgust, avoidance behavior, and physiological responses[18]. This heterogeneity can make it challenging to identify consistent neural patterns across individuals. One goal of the current research is to address this heterogeneity issue by investigating psychological dimensions relevant to spider phobia and their brain correlates.

Besides neuroimaging, it is important to investigate spider phobia at the behavioral level. First, self-report questionnaires have been shown to indicate different levels of fear of spiders[19], as well as related emotions and psychological constructs such as disgust, or state- and trait-anxiety[20–22]. Second, behavioral avoidance tests (BATs), in which spider-fearful individuals are asked to approach a spider, are important measures that can provide further insight into avoidance behavior[23–25]. More recently, some computerized versions of BATs have been developed[26,27]. Despite the availability of these measures, knowledge of how behavioral data relate to brain data is limited. This knowledge could greatly benefit clinical applications and the development of tailored interventions[28].

[1]Department of Cognition, Emotion, and Methods in Psychology, University of Vienna, Vienna, Austria. [2]These authors contributed equally: Mengfan Zhang, Alexander Karner. [3]These authors jointly supervised this work: Cindy Sumaly Lor, Frank Scharnowski. ✉e-mail: mengfan.zhang@univie.ac.at

Here, we present behavioral and MRI data of 49 individuals with fear of spiders. Specifically, we collected behavioral data consisting of a variety of self-report questionnaires that are highly relevant to fear of spiders, a physical behavioral avoidance test with a real spider, and a novel computerized behavioral avoidance test. Moreover, participants underwent an extensive MRI scan with a passive-viewing task, in which they were presented with images depicting spiders and neutral images. A resting-state scan was performed both before and after the passive-viewing task. Anatomical data were also acquired. After the MRI appointment, participants rated the spider images they had been presented with on a 101-point scale, according to "fear", "disgust" and "willingness to approach". Finally, participants underwent two follow-up assessments to examine a potential reduction in fear of spiders. As a result, the present study not only provides a large neuroimaging dataset, but also combines a broad variety of measurements, including both conventional and novel approaches. A subset of the data was analyzed (but not released) in a previous study[29]. Specifically, we used resting-state data from 37 out of 49 participants to compare functional connectivity before and after the passive-viewing task. We found decreased thalamo-cortical and increased intra-thalamic connectivity, suggesting that resting-state measures can be affected by prior emotion-inducing tasks and need to be carefully considered when detecting clinical biomarkers. The remainder of the data has not been previously used and the dataset is suitable for many questions investigating the neural mechanisms of phobias, fear processing, correlation between brain activity and phobic behavior as well as appraisal, interventions, and treatments, etc. This dataset also contributes to the growing collection of open MRI datasets, in particular, it contains neural responses from spider-fearful individuals that are relatively difficult to access. Since the original aim of the study was to examine within-subject responses to images, the SpiDa-MRI dataset does not include a control group of individuals without spider fear. As a result, the dataset has limitations in identifying markers specific to spider phobic compared to non-phobic populations. However, the inclusion criteria were set to include participants with even low levels of spider fear to ensure a wide continuum of fear severity. This allows for a range of analyses besides binary classifications, such as multivariate regression to explore neural responses across varying levels of spider fear, investigating how different fear levels influence behavioral changes, or combining our dataset with other phobic or non-phobic populations to identify common or distinct patterns. It is important to consider the sample size and effect size when performing different analyses, as some approaches, such as regression analyses, require a larger amount of data to achieve sufficient statistical power.

Methods

Participants. Fifty-one healthy, German-speaking individuals (41 female, 10 male) between the ages of 18 and 37 (mean = 22.65 ± 3.54) with self-reported fear of spiders and the willingness to overcome their fear participated in the study. Due to technical reasons, two participants had to be excluded from the dataset and the analysis, resulting in a total of 49 participants (40 female, 9 male; mean age = 22.55 ± 3.52, min = 18, max = 37). Participants were recruited via the University of Vienna's participant database, where they received an invitation and indicated their interest in participating. After signing up, they received an MRI safety questionnaire to evaluate their suitability to undergo an MRI examination and filled out the German Spider Fear Screening Questionnaires[19] (SAS; mean = 15.9 ± 4.4) where they had to score a minimum of 8 out of 24 points, indicating at least a moderate fear of spiders. Other exclusion criteria were self-reported past or current diagnosed psychiatric illnesses, pregnancy, or a history of alcohol or drug abuse. Prior to participation, all participants provided informed consent form via the SoSci platform[30], where they read the study information and needed to check a box before filling out the online survey. Additionally, on the day of the BAT and MRI scan, they provided written informed consent. In both online and onsite informed consent, we clearly explained the purpose of the study, study duration and procedures, potential risks, privacy, data use and sharing, and the participant's right to withdraw consent and stop participation at any time without any disadvantage. Participants received a financial compensation of 50€, with some receiving an additional 5€ to compensate them for a pre-participation COVID-19 testing when required by the guidelines at the time. Data were collected between September 2021 and January 2023. The study was conducted in accordance with the Declaration of Helsinki and approved by the Ethics Committee of the University of Vienna (IRB numbers: 00584, 00657).

Stimuli. The stimulus set used in the present study consisted of 225 images depicting spiders or spider-related content, and was a subset of the 313 images from a spider image database previously established by our lab (https://osf.io/vmuza/[31]). These images were rated according to the dimensions of "fear", "disgust", and "willingness to approach" by individuals with self-reported fear of spiders in a previous study[32]. To select 225 images that differed the most on these three psychological dimensions, ratings first underwent a whitening transformation to account for the different scaling of the ratings and their covariance using the "whitening" package in R[33]. Then we used the "maximin" package to make a space-filling design using 225 images under the consideration of maximum-minimum distance. Some images depicted cobwebs, cartoon spiders or small spiders, while other images showed large spiders such as tarantulas or huntsman spiders, spiders eating prey, spiders in contact with human skin, or similar. All images had a size of 800 × 600 pixels and were upscaled to 1000 × 750 pixels for the passive-viewing fMRI scan.

Experimental procedures. The experiment consisted of a set of online surveys with self-report questionnaires, a behavioral avoidance test (BAT) with an actual spider, a computerized BAT, a passive-viewing MRI scan, ratings of spider images, as well as two follow-up sessions. An overview of the experimental design is provided in Fig. 1.

Self-report questionnaires. At a time point between one and 14 days prior to the MRI appointment, participants received a link to an online questionnaire on the SoSci platform of University of Vienna, where they (similar

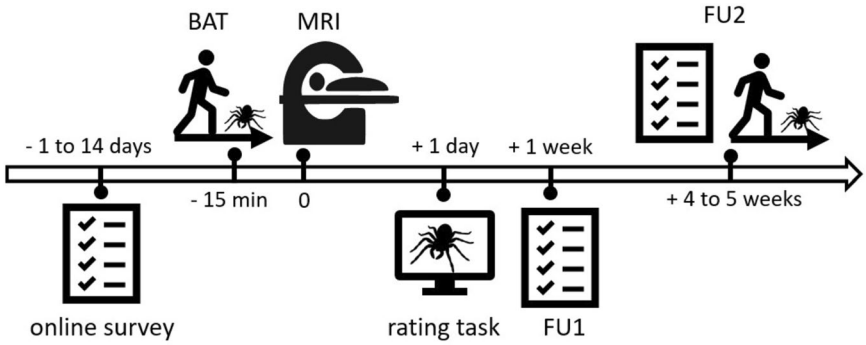

Fig. 1 Overview of the experimental design. After confirming eligibility for participation in the study, participants received a link to an online survey with self-report questionnaires, that was filled out between 1 and 14 days prior to the MRI appointment. On the day of the MRI appointment, participants underwent a behavioral avoidance test (BAT) with a spider and a computerized BAT. Approximately 15 minutes after completing the BATs, they started the MRI appointment, during which they were presented with spider images on a screen. One day after the MRI appointment, participants received a link to an online image rating task, in which they rated the images they had been presented with according to "fear", "disgust", and "willingness to approach". One week after the MRI appointment, participants engaged in a brief online follow-up (FU1), where they filled out a self-report questionnaire. Between four and five weeks after the MRI appointment, participants underwent a second follow-up (FU2), which consisted of a self-report questionnaire, a BAT, and a computerized BAT.

to Karner *et al.*[32]) answered self-report questionnaires indicating their level of fear of spiders, specifically the German validated versions of the Fear of Spiders Questionnaire (FSQ)[34] and the Spider Phobia Questionnaire[35], that where introduced by Rinck *et al.*, together with the German Spider Screening[19]. Additionally, participants filled out questionnaires indicating state- and trait anxiety (STAI)[20], disgust propensity (FEE)[21], and disgust sensitivity (SEE)[22]. Demographic information was also collected.

Behavioral avoidance test. On the day of the MRI appointment, participants came to the University of Vienna, where they underwent a BAT, in which they were asked to approach a terrarium containing a spider. The spider was a real huntsman spider (*Heteropoda ssp.;* Latreille, 1804), which was inanimate and prepared in a natural-looking position. Participants were unaware that the spider was not alive. Before entering the room with the terrarium, they received the following instructions from the experimenter: *"In this room, we have a terrarium containing a spider. We would like to ask you to approach the terrarium up until a point where you still feel comfortable, and then stop and let us know. If you want to go all the way to the terrarium and feel comfortable, you may open the transparent lid, but you don't have to do this."* (translated from German) Then, the experimenter opened the door to the room with the terrarium and asked the participants to position their right foot behind a cross on the floor, which was 4.5 meters away from the terrarium. The experimenter remained standing in the door frame. While participants approached the terrarium, the distance covered was measured in centimeters using a laser distance meter that was always positioned in the same predefined spot and directed towards the participants' leg. Specifically, we measured the start and end distance, to calculate the net distance that participants walked towards the terrarium. Two different terrariums (terrarium *A* and terrarium *B*) with identical spiders, but slightly different interior was used within the scope of the study to prevent potential biases due to static mental representations of the terrarium. Approximately half of the participants approached terrarium *A* on the day of the MRI appointment and terrarium *B* on the day of the follow-up appointment, and vice versa.

Computerized behavioral avoidance test. In addition to the BAT, participants underwent a novel computerized BAT (cBAT) that was designed based on the work of Peirce *et al.*[36] and implemented in PsychoPy (available at: https://osf.io/vmuza/[31]). In this task, participants needed to sharpen three highly blurred images of spiders up until a point where they still felt comfortable looking at them by dragging a slider on the screen. Although the scale was linear, with values from 1 to 101 stored, the sharpening of the images occurred in a logarithmic manner. At the start of the cBAT, participants read the following instructions on the screen: *"On the following pages, you will see blurred, unrecognizable images of spiders. Use the slider to sharpen each image to the point where you still feel comfortable looking at it. Important: Keep the left mouse button pressed while moving the slider. As soon as you release the left mouse button, your answer will be saved. We will start with a practice round with a neutral image. This will be followed by the spider images. If you want to start, press the Space key."* (translated from German) The practice image consisted of a chair on a wooden floor, followed by three spider images displaying relatively large spiders. Contrary to the BAT, the experimenter left the room while participants engaged in the cBAT. However, in a subset of the cBATs (labeled in the BAT.csv file in the behavioral data), the experimenter remained present in the room with the participant. The order of performing the BAT first or the cBAT first was counterbalanced.

Passive-viewing mri scan. After completing the BAT and cBAT, participants underwent a brain scan at the University of Vienna's MR Center. To reduce head motion, an easily removable, non-constrictive piece of tape was placed on the participant's forehead to provide tactile feedback as described by Krause *et al.*[37]. Stimuli were presented to participants on an MR-compatible LCD screen (BOLDscreen 32 LCD for fMRI, Cambridge Research Systems) that was positioned at the head of the scanner bore. Participants were able to view the screen through a mirror mounted onto the head coil. First, a resting-state scan was performed during which participants were instructed to relax and keep their eyes open and directed at a fixation point. Subsequently, participants engaged in a passive-viewing task that consisted of five runs. In each run, participants were presented with 45 spider images, which displayed spiders and spider-related content, as well as with 15 neutral images depicting inanimate objects. Each image presentation lasted for four seconds and was followed by a presentation of the fixation point for two to three seconds. All images had a size of 1000 × 750 pixels. In each run, participants also underwent 6 catch trials, in which they were instructed to press a specific button on a button box that was positioned in their hand (e.g. *"Please press the left button now."*). Once a catch trial was completed, the next image was presented to the participant. As an additional attention check, the experimenters used the live video of an eye tracker to see whether participants were keeping their eyes open, which was communicated to the participants beforehand. After runs 1, 3, and 5, participants were asked about their current levels of agitation and exhaustion, which they stated via the intercom on a scale from 0 to 10. All measurements in the scanner were made consecutively. The five passive-viewing runs were followed by another resting-state scan which was identical to the first resting-state scan. This was followed by a structural scan, which marked the end of the scanning session. The MRI data therefore consists of seven functional runs, five passive viewing runs, and two resting state runs, as well as a structural scan.

Image ratings. One day after the MRI appointment, participants received an email with links to the University of Vienna's SoSci platform, where they were asked to rate all spider images that had been presented to them during the passive viewing fMRI scan. The ratings were divided into three blocks (A, B, and C), each containing 75 images, with the order of block completion counterbalanced. The images were presented in their original size of 800 × 600 pixels. Participants were allowed to take breaks between the blocks, with the requirement to complete all three blocks within 48 hours after receiving the links. However, the research team also accepted ratings made a week or more after the fMRI appointment. The image rating procedure was based on the study by Karner *et al.*[32]. Each block started with a practice round, followed by the actual image ratings. In each image rating trial, an image was presented on the screen for three seconds. Then the image disappeared, and three questions and corresponding rating scales appeared on the screen. (1) "How much fear does this picture elicit in you?"; (2) "How much disgust does this picture elicit in you?"; (3) "How close could you come to the content shown in the picture, if you wanted to overcome your aversion?" (translated from German). Ratings were made via a continuously adjustable slider on a 101-point visual analog scale. In each trial, participants had 12 seconds to administer the three ratings. To proceed with the next image, they clicked "Next" in the bottom-right corner on the screen. Each block contained a break questionnaire[32], in which participants stated their current levels of fear, physical arousal, disgust, boredom, and exhaustion in subjective units of distress[38] on a scale from 0–10. Additionally, each break questionnaire contained a bogus item to test the participants' attention[39].

Follow-up assessments. One week after the MRI appointment, participants received a link to an online questionnaire where they were asked to fill out the FSQ a second time (follow-up 1). A total of 41 out of 49 participants completed follow-up 1. Follow-up 2 took place between four and five weeks after the MRI appointment. Participants returned to the University of Vienna, where they first filled out the FSQ a third time and then completed the BAT and cBAT for a second time. Thirteen participants filled out the FSQ after having completed the BAT and cBAT. Participants were then asked to fill out a brief feedback sheet asking them about their thoughts on the study, and whether they noticed anything special. A total of 46 out of 49 participants completed follow-up 2. Out of all the participants, only one person expressed doubt about the authenticity of the spider. The feedback sheet marked the end of the participation in the experiment.

MRI acquisition. All functional and structural scans were collected using a 3T Siemens MAGNETOM Skyra MRI scanner (Siemens, Erlangen, Germany) with a 32-channel head coil, located at the University of Vienna. Functional data were acquired with an interleaved mode, using a T2*-weighted echo planar imaging sequence with multiband acceleration factor 4, bandwidth = 1796 Hz/Px, TR = 1250 ms, TE = 36 ms, voxel size = 2 mm * 2 mm * 2 mm, flip angle = 65 degrees, field of view (FOV) = 192 mm * 192 mm * 145 mm, 56 slices without slice gap to cover the full brain, and anterior-posterior phase encoding. The total scan duration for each resting state run was 9:00 mins, and 7:20 mins for each passive viewing run. After the functional runs, a field map was collected with a short echo time of 4.92 ms and a long echo time of 7.38 ms.

Structural data for each participant was acquired using a single-shot, high-resolution MPRAGE sequence with an acceleration factor of 2 using GRAPPA with bandwidth = 200 Hz/Px, TR = 2300 ms, TE = 2.43 ms, voxel size = 0.8 mm * 0.8 mm * 0.8 mm, flip angle = 8 degrees, and field of view (FOV) = 263 mm * 350 mm * 350 mm. The total duration of the structural data acquisition was 6:35 mins.

MRI preprocessing. *Data anonymization and raw data standardization.* Participants were assigned a randomly generated 6-character combination of numbers and letters as their identifier (e.g., ac9rnl) for all experiments. First, we replaced the 6-character identifier with a subject numeric identifier (e.g., sub-03) so that participants would not be able to look up their own files in our dataset. Second, we organized the Siemens scanner output data into the Brain Imaging Data Structure (BIDS)[40] specification (version 1.0.1) format using a self-developed script that included the process of converting data from DICOM format to NIfTI format using

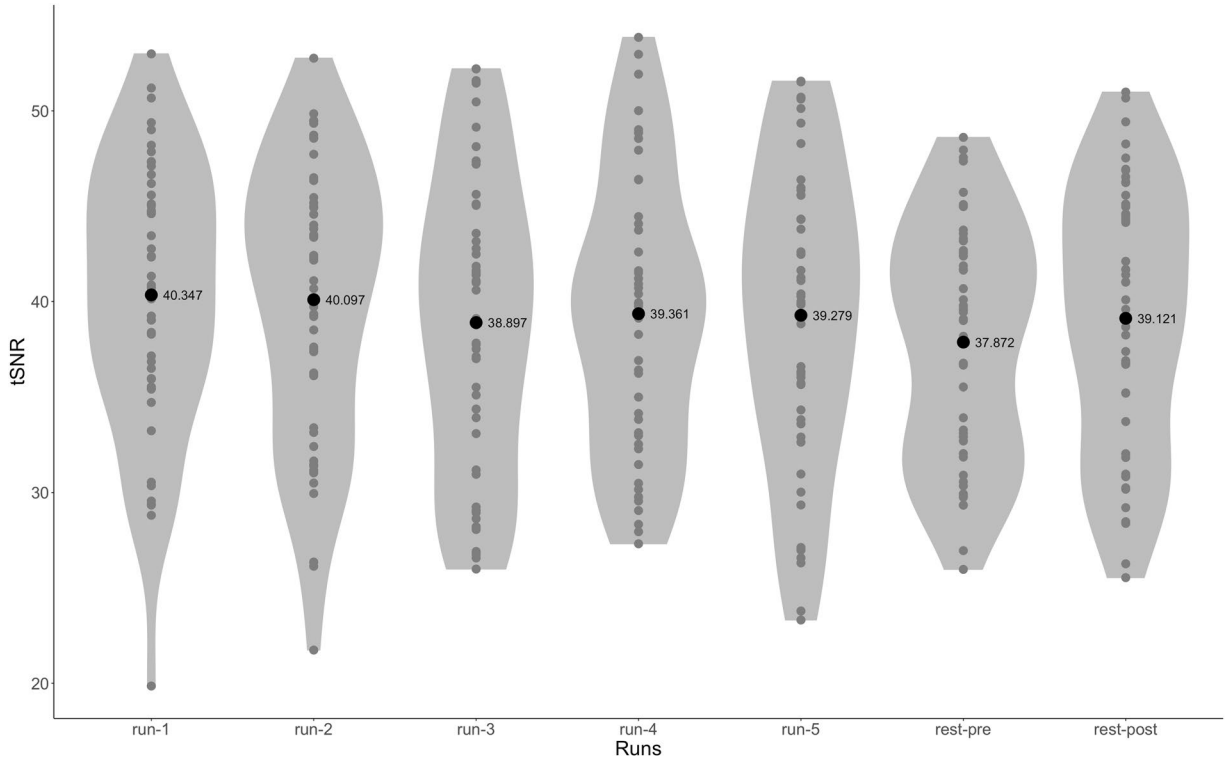

Fig. 2 Temporal SNR of each run across all participants. Gray dots represent the individual tSNR for that run. Black dots and associated values are the mean tSNR across all participants for that run. The mean whole-brain tSNR across participants for all runs was 39.28 ± 7.20.

dcm2nii software[41], extracting relevant metadata into JSON files, generating event TSV files from stimulus presentations, and renaming files according to the BIDS specification. Third, we used the PyDeface package[42] to remove facial structures from the T1-weighted anatomical images. Finally, we visually inspected the defaced images to confirm that the faces had been removed, while the brains were preserved in all images.

The resulting data from the anonymization and standardization were validated using the online bids-validator software (https://bids-standard.github.io/bids-validator/[43]). Two warnings were issued to indicate potential problems. The first warning: "Not all subjects/sessions/runs have the same scan parameters." was caused by a technical problem during the data transfer. The 290th DICOM volume (out of 345) corresponding to the 56th trial (out of 66) in the first passive-viewing run of subject sub-07 (sub-07/func/sub-07_task-passiveview_run-1_bold.nii) failed to be transferred from the Siemens scanner, leaving the run contains 344 volumes instead of 345. Importantly, this missing volume requires careful handling during data analysis, either with interpolation, censoring, exclusion of the trial, or exclusion of the entire run. The second warning: "The start of the last event is after the total duration of the corresponding scan. This design is suspiciously long." was caused by the fact that the length of the experiment depended on how fast the participants pressed the buttons during catch trials. The length of the scanning acquisition was set to 345 volumes per passive-viewing run and was largely sufficient for all the participants except for two (sub-08 and sub-20). For the 3rd run of these two participants, the data acquisition stopped before the last two images were presented. This should carefully be taken into consideration for any future analysis, either by excluding the runs or by adjusting the analysis to exclude the last two images.

Anatomical data preprocessing. The pre-processed anatomical and functional data included in this dataset was performed with fMRIPrep 20.2.6[44], which is based on Nipype 1.7.0[45].

The T1-weighted (T1w) images were first corrected for intensity non-uniformity (INU) using N4BiasFieldCorrection[46], and used as T1w-reference throughout the workflow. Then, the T1w-reference was skull-stripped with antsBrainExtraction.sh workflow, using OASIS30ANTs as the target template. Brain tissue segmentation of cerebrospinal fluid (CSF), white matter (WM), and gray matter (GM) was performed on the brain-extracted T1w using the software fast (FSL 5.0.9, RRID:SCR_002823[47]). Volume-based spatial normalization to the standard space (MNI152NLin2009cAsym) was performed through nonlinear registration using antsRegistration (ANTs 2.3.3), with brain-extracted versions of both T1w reference and T1w template.

Functional data preprocessing. For each of the seven functional runs per subject, the following procedures were performed: First, a reference volume and its skull-stripped version were generated using a custom methodology of fMRIPrep. A B_0-nonuniformity map (i.e. fieldmap) was estimated based on a phase-difference map calculated with a dual-echo GRE (gradient-recall echo) sequence, processed with a custom workflow of SDCFlows. The field map was then co-registered to the target EPI (echo-planar imaging) reference run

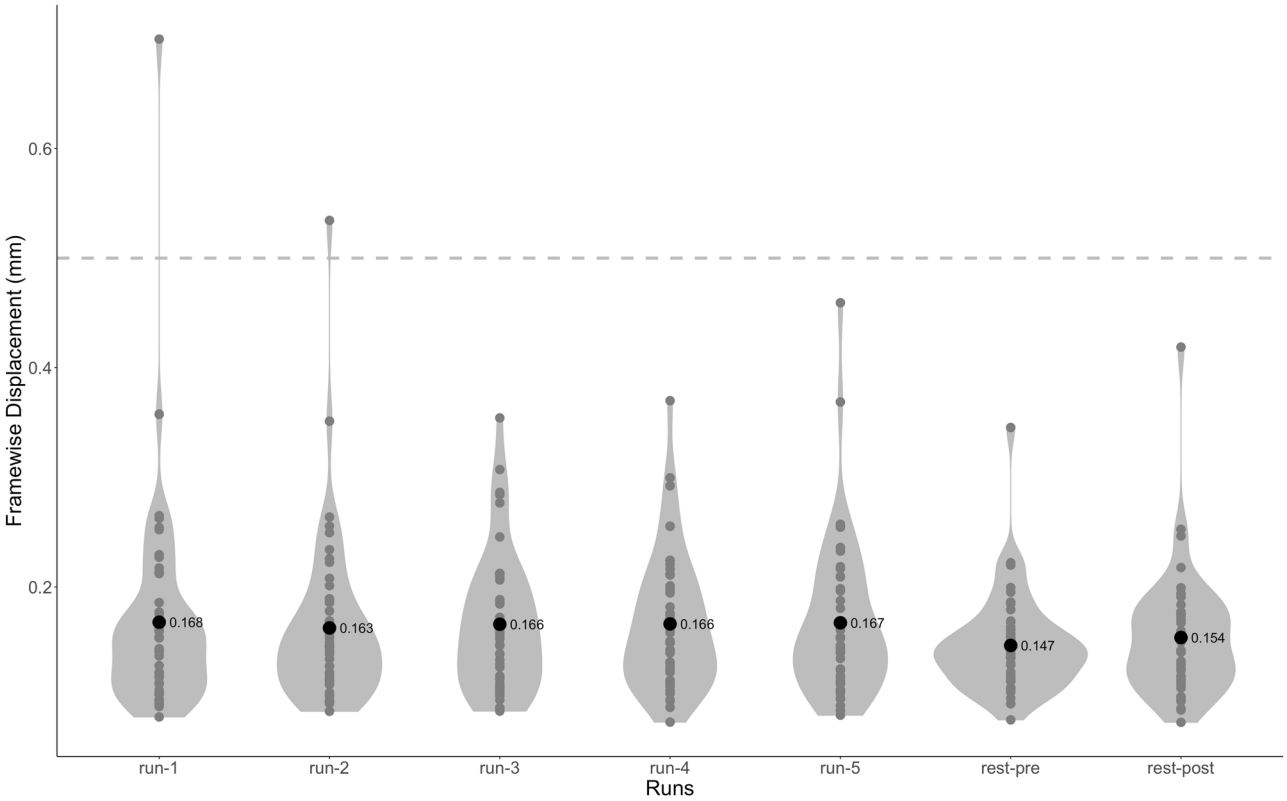

Fig. 3 Framewise displacement of each run across all participants. Gray dots represent the individual FD for that run. Black dots and associated values are the mean FD across all participants for that run. Participant movement is low in this dataset, only two runs of one participant had higher than 0.5 mm FD. The mean FD across participants for all runs was 0.16 ± 0.07 mm.

and converted to a displacement field map with FSL's fugue and other SDCFlows tools. Based on the estimated susceptibility distortion, a corrected EPI reference was calculated for a more accurate co-registration with the anatomical reference. The reference was then co-registered to the T1w reference using flirt, and the co-registration was configured with nine degrees of freedom to account for distortions remaining in the reference. Head-motion parameters (transformation matrices, and six corresponding rotation and translation parameters) were estimated before any spatiotemporal filtering using mcflirt[48]. BOLD runs were slice-time corrected to 0.571 s using 3dTshift[49]. The fMRI time-series were resampled onto their original, native space by applying a single, composite transform to correct for head-motion and susceptibility distortions. Also, the fMRI time-series were resampled into standard space, generating a preprocessed functional run in the MNI152NLin2009cAsym space. Several confounding time-series were calculated based on the preprocessed BOLD: framewise displacement (FD), DVARS, and three region-wise global signals. FD and DVARS were calculated for each functional run, both using their implementations in Nipype, and the three global signals were extracted within the CSF, the WM, and the whole-brain masks. Additionally, a set of physiological regressors was extracted to allow for component-based noise correction (CompCor)[50]. Principal components were estimated after high-pass filtering the preprocessed fMRI time-series for the two CompCor variants: temporal (tCompCor) and anatomical (aCompCor). tCompCor components were then calculated from the top 2% variable voxels within the brain mask. For aCompCor, three probabilistic masks (CSF, WM and combined CSF + WM) were generated in anatomical space. From these masks, a mask of voxels likely to contain a volume fraction of GM was subtracted and then resampled in BOLD space. The head-motion estimates calculated in the correction step were also placed within the corresponding confounds files. All resamplings were performed with a single interpolation step by composing all the pertinent transformations. (i.e. head-motion transform matrices, susceptibility distortion correction when available, and co-registrations to anatomical and output spaces). Gridded (volumetric) resamplings were performed using antsApplyTransforms (ANTs), configured with Lanczos interpolation to minimize the smoothing effects of other kernels[51]. Non-gridded (surface) resamplings were performed using mri_vol2surf (FreeSurfer).

Many internal operations of fMRIPrep use Nilearn 0.6.2[52] (RRID:SCR_001362), mostly within the functional processing workflow. For more details of the pipeline, see the section corresponding to workflows in fMRIPrep's documentation (https://fmriprep.org/en/20.2.6/workflows.html).

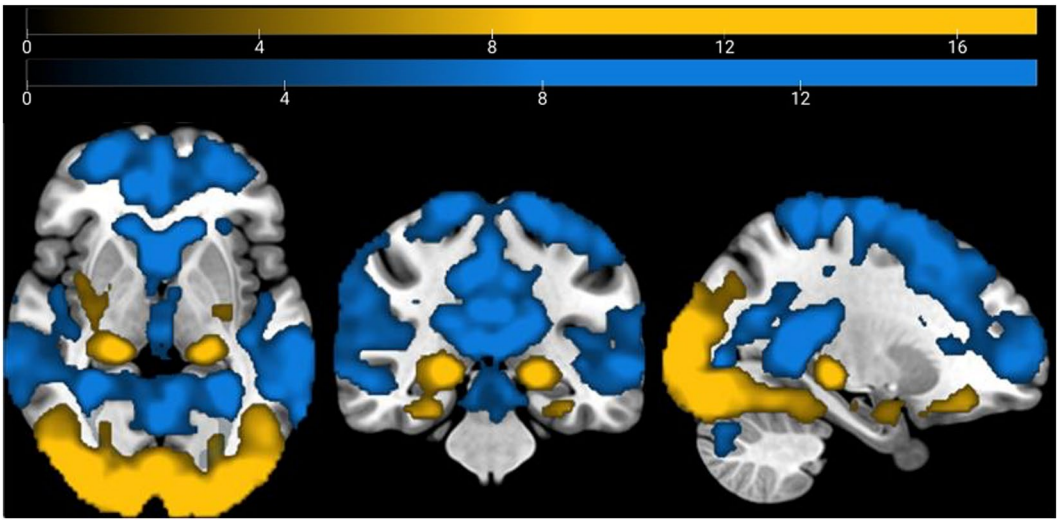

Fig. 4 Brain activation clusters for stimulus presentation vs. implicit baseline ($p < 0.001$ for peak threshold and $p < 0.05$ for FWE-cluster correction). Blue: negative activation; yellow: positive activation. $N = 49$.

Data Records

Data from SpiDa-MRI can be subdivided into the behavioral and neuroimaging datasets. The behavioral data, including self-report questionnaires, BAT and cBAT distances, ratings of spider images, and the corresponding README file and codebooks with value labels are available on OSF (https://osf.io)[53] at https://osf.io/w4s2h/[54].

All neuroimaging data is organized according to BIDS specification (version 1.0.1) and is openly available via OpenNeuro (https://openneuro.org)[55] at https://openneuro.org/datasets/ds004630[56]. The raw subject-level data can be found under the directory "sub-xx" (e.g., sub-03) which consists of "func" (for functional images and event log files of passive-viewing runs), "fmap" (for field map images) and "anat" (for defaced anatomical images) sub-directories. Pre-processed data with fMRIprep version 20.2.6[44] can be found under the "derivatives/fmriprep" directory. For each subject, the 'desc-confounds_timeseries.tsv' files located within this directory contain various confound regressors essential for further analysis. These include motion parameters, global signal, CSF signal, white matter signal, and additional parameters such as framewise displacement, DVARS, and CompCor components. Quality assessment reports with MRIQC version 21.0.0rc2[57] can be found under the "derivative/mriqc" directory. All 3D or 4D MRI data is stored in "NIFTI" (extension: nii) or compressed "NIFTI" files (extension: nii.gz) with its associated metadata in JSON files.

Technical Validation

Quality assessment. To assess the quality of the current dataset, we used an open-source BIDS application, MRIQC[57], to automatically generate Image Quality Metrics (IQMs) and visual quality reports for individual and group levels. Following the developers' recommendation for the MRIQC software, IQMs were calculated before defacing and preprocessing to accurately assess the quality of the original data and prevent bias[58]. Individual functional reports were generated per subject per run to show the mosaic view of the average BOLD signal map, standard deviation from the average BOLD signal map, summary plot of motion-related indices, and IQMs. The IQMs include commonly used measures of spatial and temporal signal quality (e.g., signal-to-noise ratio (SNR), temporal SNR (tSNR, Fig. 2), DVARS) and measures of artifacts (e.g., framewise displacement (FD, Fig. 3), number of dummy scans). The individual anatomical reports include a mosaic zoomed-in brain mask map, a background noise map, and IQMs including noise measurements. The group functional and anatomical reports visualize the IQMs across participants by displaying a box plot per measure. These reports graphically show the range and outliers of quality measures and can be used to quickly compare participants. All reports and accompanying JSON and TSV files are shared on OpenNeuro.

Basic analysis of stimuli vs. implicit baseline. To further validate the dataset, we performed a basic general linear model (GLM) analysis to show brain activation during stimulus presentation compared to an implicit baseline. This analysis should find positive voxel activation in visual areas and task-related regions, such as the hippocampus and the amygdala. For this purpose, we used the fMRIprep-preprocessed passive-viewing functional scans and Statistical Parametric Mapping (SPM12; Wellcome Trust Centre for Neuroimaging, London, United Kingdom) for the GLM analysis. Runs for which the maximum framewise displacement (FD) exceeded 5 mm were excluded from the analysis (2 runs of one participant). For the first-level analysis, we specified two regressors, one for the onsets of stimulus presentation (including spider images and neutral images) and one for the onsets of the button-press catch trials. Each stimulus was modeled as a boxcar function, with lengths matching each stimulus duration, and convolved with the hemodynamic response function. The six motion realignment parameters were added as nuisance regressors. We performed a one-sample t-test second-level analysis, one for positive activation and one for negative activation, using the first-level activation maps that correspond

to the "stimuli" regressor from the 49 participants. We applied a family-wise error corrected cluster threshold of $p < 0.05$, with the height threshold set at $p < 0.001$. As expected, we found positive activation in visual areas, as well as fear-related regions such as the bilateral amygdala, hippocampus, and putamen. Conversely, we found negative activation in regions associated with resting-state such as parts of the default-mode network among other regions (Fig. 4). This outcome is consistent with the previous literature on similar experimental paradigms[59].

Code availability

All code is available in the GitHub repository (https://github.com/univiemops/spider20-fmri-data). The code includes scripts for experiment presentation (executed in Python and largely relied on PsychoPy), data sorting, preprocessing and quality control (executed in shell scripting), and analyses (executed in Matlab).

Received: 24 June 2024; Accepted: 31 January 2025;
Published online: 17 February 2025

References

1. Marks, I. M. *Fears, Phobias, and Rituals: Panic, Anxiety, and Their Disorders*. (Oxford University Press, 1987).
2. Wardenaar, K. J. *et al*. The cross-national epidemiology of specific phobia in the World Mental Health Surveys. *Psychol. Med.* **47**, 1744–1760 (2017).
3. American Psychiatric Association. *Diagnostic and Statistical Manual of Mental Disorders: DSM-5™, 5th edn*. (American Psychiatric Publishing, 2013).
4. Fredrikson, M., Annas, P., Fischer, H. & Wik, G. Gender and age differences in the prevalence of specific fears and phobias. *Behav. Res. Ther.* **34**, 33–39 (1996).
5. Oosterink, F. M. D., De Jongh, A. & Hoogstraten, J. Prevalence of dental fear and phobia relative to other fear and phobia subtypes. *Eur. J. Oral Sci.* **117**, 135–143 (2009).
6. Zsido, A. N. The spider and the snake – A psychometric study of two phobias and insights from the Hungarian validation. *Psychiatry Res.* **257**, 61–66 (2017).
7. Hinze, J. *et al*. Spider Phobia: Neural Networks Informing Diagnosis and (Virtual/Augmented Reality-Based) Cognitive Behavioral Psychotherapy-A Narrative Review. *Front. Psychiatry* **12**, 704174 (2021).
8. Holzschneider, K. & Mulert, C. Neuroimaging in anxiety disorders. *Dialogues Clin. Neurosci.* **13**, 453–461 (2011).
9. Davey, G. C. L. The 'Disgusting' Spider: The Role of Disease and Illness in the Perpetuation of Fear of Spiders. *Soc. Anim.* **2**, 17–25 (1994).
10. Gerdes, A. B. M., Uhl, G. & Alpers, G. W. Spiders are special: fear and disgust evoked by pictures of arthropods. *Evol. Hum. Behav.* **30**, 66–73 (2009).
11. Olatunji, B. O. & McKay, D. Further exploration of the role of disgust sensitivity in anxiety and related disorders. *Anxiety Stress Coping* **19**, 331–334 (2006).
12. Stark, R. *et al*. Hemodynamic brain correlates of disgust and fear ratings. *NeuroImage* **37**, 663–673 (2007).
13. Solarz, A. K. Latency of instrumental responses as a function of compatibility with the meaning of eliciting verbal signs. *J. Exp. Psychol.* **59**, 239–245 (1960).
14. Lewin, K. *A Dynamic Theory of Personality*. (1935).
15. Zorowitz, S. *et al*. The Neural Basis of Approach-Avoidance Conflict: A Model Based Analysis. *eNeuro* **6**, ENEURO.0115-19.2019 (2019).
16. Rosenbaum, D. *et al*. Neuronal correlates of spider phobia in a combined fNIRS-EEG study. *Sci. Rep.* **10**, 12597 (2020).
17. Knopf, K. & Pössel, P. Individual response differences in spider phobia: comparing phobic and non-phobic women of different reactivity levels. *Anxiety Stress Coping* **22**, 39–55 (2009).
18. Schienle, A., Schäfer, A., Walter, B., Stark, R. & Vaitl, D. Brain activation of spider phobics towards disorder-relevant, generally disgust- and fear-inducing pictures. *Neurosci. Lett.* **388**, 1–6 (2005).
19. Rinck, M. *et al*. Reliabilität und Validität dreier Instrumente zur Messung von Angst vor Spinnen. *Diagnostica* **48**, 141–149 (2002).
20. Laux, L., Glanzmann, P. G., Schaffner, P. & Spielberger, C. D. *Das State-Trait-Angstinventar STAI; Theoretische Grundlagen Und Handanweisung*. (Beltz Test, Weinheim, 1981).
21. Schienle, A., Walter, B., Stark, R. & Vaitl, D. Ein Fragebogen zur Erfassung der Ekelempfindlichkeit (FEE). *Z. Für Klin. Psychol. Psychother.* **31**, 110–120 (2002).
22. Schienle, A., Dietmaier, G., Ille, R. & Leutgeb, V. Eine Skala zur Erfassung der Ekelsensitivität (SEE). *Z. Für Klin. Psychol. Psychother.* **39**, 80–86 (2010).
23. Antony, M. M. & Swinson, R. P. *Phobic Disorders and Panic in Adults: A Guide to Assessment and Treatment*. xii, 422 https://doi.org/10.1037/10348-000 (American Psychological Association, 2000).
24. Muris, P., Merckelbach, H., Holdrinet, I. & Sijsenaar, M. Behavioral Avoidance Test. https://doi.org/10.1037/t11195-000 (1998).
25. Öst, L.-G., Salkovskis, P. M. & Hellström, K. One-session therapist-directed exposure vs. self-exposure in the treatment of spider phobia. *Behav. Ther.* **22**, 407–422 (1991).
26. Grill, M., Heller, M. & Haberkamp, A. *Development and Validation of an Open-Access Online Behavioral Avoidance Test (BAT) for Spider Fear*. (2023).
27. Mühlberger, A., Neumann, R., Wieser, M. J. & Pauli, P. The impact of changes in spatial distance on emotional responses. *Emot. Wash. DC* **8**, 192–198 (2008).
28. McNally, R. J. Mechanisms of exposure therapy: How neuroscience can improve psychological treatments for anxiety disorders. *Clin. Psychol. Rev.* **27**, 750–759 (2007).
29. Lor, C. S. *et al*. Pre- and post-task resting-state differs in clinical populations. *NeuroImage Clin.* **37**, 103345 (2023).
30. Leiner, D. J. SoSci survey (version 3.1. 06). (2019).
31. Scharnowski, F. spider stimuli. https://doi.org/10.17605/OSF.IO/VMUZA (2024)
32. Karner, A. *et al*. The "SpiDa" dataset: Self-report questionnaires and ratings of spider images from spider-fearful individuals. *Front. Psychol.* **15**, 1327367 (2024).
33. R Core Team. R: A Language and Environment for Statistical Computing. R Foundation for Statistical Computing (2023).
34. Szymanski, J. & O'Donohue, W. Fear of Spiders Questionnaire. *J. Behav. Ther. Exp. Psychiatry* **26**, 31–34 (1995).
35. Watts, F. N. & Sharrock, R. Questionnaire dimensions of spider phobia. *Behav. Res. Ther.* **22**, 575–580 (1984).
36. Peirce, J. *et al*. PsychoPy2: Experiments in behavior made easy. *Behav. Res. Methods* **51**, 195–203 (2019).
37. Krause, F. *et al*. Active head motion reduction in magnetic resonance imaging using tactile feedback. *Hum. Brain Mapp.* **40**, 4026–4037 (2019).
38. Wolpe, J. *The Practice of Behavior Therapy*. (Pergamon Press, 1969).
39. Meade, A. W. & Craig, S. B. Identifying careless responses in survey data. *Psychol. Methods* **17**, 437–455 (2012).

40. Gorgolewski, K. J. *et al*. The brain imaging data structure, a format for organizing and describing outputs of neuroimaging experiments. *Sci. Data* **3**, 160044 (2016).
41. Li, X., Morgan, P. S., Ashburner, J., Smith, J. & Rorden, C. The first step for neuroimaging data analysis: DICOM to NIfTI conversion. *J. Neurosci. Methods* **264**, 47–56 (2016).
42. Gulban, O. F. *et al*. poldracklab/pydeface: PyDeface v2.0.2. Zenodo https://doi.org/10.5281/zenodo.6856482 (2022).
43. bids-standard/bids-validator. Brain Imaging Data Structure (2024).
44. Esteban, O. *et al*. fMRIPrep: a robust preprocessing pipeline for functional MRI. *Nat. Methods* **16**, 111–116 (2019).
45. Gorgolewski, K. *et al*. Nipype: A Flexible, Lightweight and Extensible Neuroimaging Data Processing Framework in Python. *Front. Neuroinformatics* **5**, 13 (2011).
46. Tustison, N. J. *et al*. N4ITK: Improved N3 Bias Correction. *IEEE Trans. Med. Imaging* **29**, 1310–1320 (2010).
47. Zhang, Y., Brady, M. & Smith, S. Segmentation of brain MR images through a hidden Markov random field model and the expectation-maximization algorithm. *IEEE Trans. Med. Imaging* **20**, 45–57 (2001).
48. Jenkinson, M., Bannister, P., Brady, M. & Smith, S. Improved Optimization for the Robust and Accurate Linear Registration and Motion Correction of Brain Images. *NeuroImage* **17**, 825–841 (2002).
49. Cox, R. W. & Hyde, J. S. Software tools for analysis and visualization of fMRI data. *NMR Biomed.* **10**, 171–178 (1997).
50. Behzadi, Y., Restom, K., Liau, J. & Liu, T. T. A component based noise correction method (CompCor) for BOLD and perfusion based fMRI. *NeuroImage* **37**, 90–101 (2007).
51. Lanczos, C. A Precision Approximation of the Gamma Function. *J. Soc. Ind. Appl. Math. Ser. B Numer. Anal.* **1**, 86–96 (1964).
52. Abraham, A. *et al*. Machine learning for neuroimaging with scikit-learn. *Front. Neuroinformatics* **8**, 14 (2014).
53. Foster, E. D. & Deardorff, A. Open Science Framework (OSF). *J. Med. Libr. Assoc. JMLA* **105**, 203–206 (2017).
54. Zhang, M. & Karner, A. SpiDa-MRI-behavioral dataset. https://doi.org/10.17605/OSF.IO/W4S2H. (2024).
55. Markiewicz, C. J. *et al*. The OpenNeuro resource for sharing of neuroscience data. *eLife* **10**, e71774.
56. Zhang, M. *et al*. SpiDa-MRI-neuroimaging dataset - OpenNeuro. https://openneuro.org/datasets/ds004630. (2024).
57. Esteban, O. *et al*. MRIQC: Advancing the automatic prediction of image quality in MRI from unseen sites. *PLOS ONE* **12**, e0184661 (2017).
58. Provins, C. *et al*. Defacing biases manual and automated quality assessments of structural MRI with MRIQC. Preprint at https://doi.org/10.31219/osf.io/t9ehk (2023).
59. Botvinik-Nezer, R. *et al*. fMRI data of mixed gambles from the Neuroimaging Analysis Replication and Prediction Study. *Sci. Data* **6**, 106 (2019).

Acknowledgements

FM was funded by the Austrian Science Fund (FWF) [10.55776/ESP133]. KK was funded by the Austrian Science Fund (FWF) [10.55776/ESP286]. FS was supported by the Swiss National Science Foundation (BSSG10_155915, 100014_178841, 32003B_166566), the Foundation for Research in Science and the Humanities at the University of Zurich (STWF-17-012), and the Baugarten Stiftung. Open access funding provided by University of Vienna.

Author contributions

M.Z.: Conceptualization, Formal Analysis, Investigation, Data Curation, Validation, Visualization, Writing - Original Draft. A.K.: Conceptualization, Methodology, Software, Formal Analysis, Investigation, Data Curation, Writing - Original Draft. K.K.: Conceptualization, Data Curation, Writing - Review & Editing. S.S.: Investigation, Writing - Review & Editing. D.S.: Conceptualization, Writing - Review & Editing. R.S.: Methodology, Resources, Writing - Review & Editing. F.M.: Software, Writing - Review & Editing. C.L.: Conceptualization, Methodology, Software, Validation, Formal Analysis, Investigation, Data Curation, Writing - Original Draft. F.S.: Conceptualization, Project Administration, Methodology, Supervision, Funding Acquisition, Resources, Writing - Review & Editing.

Competing interests

The authors declare no competing interests.

Additional information

Correspondence and requests for materials should be addressed to M.Z.

Reprints and permissions information is available at www.nature.com/reprints.

Publisher's note Springer Nature remains neutral with regard to jurisdictional claims in published maps and institutional affiliations.